RADIATION RESEARCH **183**, 357–366 (2015)
0033-7587/15 $15.00

DOI: 10.1667/RR13915.1

A Tocotrienol-Enriched Formulation Protects against Radiation-Induced Changes in Cardiac Mitochondria without Modifying Late Cardiac Function or Structure

Vijayalakshmi Sridharan,[a,1] Preeti Tripathi,[a] Nukhet Aykin-Burns,[a] Kimberly J Krager,[a] Sunil K. Sharma,[b] Eduardo G. Moros,[c] Stepan B. Melnyk,[d] Oleksandra Pavliv,[d] Martin Hauer-Jensen[a,e] and Marjan Boerma[a]

[a] *University of Arkansas for Medical Sciences, Department of Pharmaceutical Sciences, Division of Radiation Health, Little Rock, Arkansas;* [b] *University of Arkansas for Medical Sciences, Department of Radiation Oncology, Little Rock, Arkansas;* [c] *Moffitt Cancer Center and Research Institute, Department of Radiation Oncology, Tampa, Florida;* [d] *University of Arkansas for Medical Sciences, Department of Pediatrics, Little Rock Arkansas; and* [e] *Surgical Service, Central Arkansas Veterans Healthcare System, Little Rock, Arkansas*

Sridharan, V., Tripathi, P., Aykin-Burns, N., Krager, K. J., Sharma, S. K., Moros, E. G., Melnyk, S. B., Pavliv, O., Hauer-Jensen, M. and Boerma, M. A Tocotrienol-Enriched Formulation Protects against Radiation-Induced Changes in Cardiac Mitochondria without Modifying Late Cardiac Function or Structure. *Radiat. Res.* 183, 357–366 (2015).

Radiation-induced heart disease (RIHD) is a common and sometimes severe late side effect of radiation therapy for intrathoracic and chest wall tumors. We have previously shown that local heart irradiation in a rat model caused prolonged changes in mitochondrial respiration and increased susceptibility to mitochondrial permeability transition pore (mPTP) opening. Because tocotrienols are known to protect against oxidative stress-induced mitochondrial dysfunction, in this study, we examined the effects of tocotrienols on radiation-induced alterations in mitochondria, and structural and functional manifestations of RIHD. Male Sprague-Dawley rats received image-guided localized X irradiation to the heart to a total dose of 21 Gy. Twenty-four hours before irradiation, rats received a tocotrienol-enriched formulation or vehicle by oral gavage. Mitochondrial function and mitochondrial membrane parameters were studied at 2 weeks and 28 weeks after irradiation. In addition, cardiac function and histology were examined at 28 weeks. A single oral dose of the tocotrienol-enriched formulation preserved Bax/Bcl2 ratios and prevented mPTP opening and radiation-induced alterations in succinate-driven mitochondrial respiration. Nevertheless, the late effects of local heart irradiation pertaining to myocardial function and structure were not modified. Our studies suggest that a single dose of tocotrienols protects against radiation-induced mitochondrial changes, but these effects are not sufficient against long-term alterations in cardiac function or remodeling. © 2015 by Radiation Research Society

INTRODUCTION

Exposure of the heart during radiotherapy poses increased risk for developing radiation-induced heart disease (RIHD), which is of concern in long-term cancer survivors (*1, 2*). Indicators of RIHD include conduction abnormalities, injury to cardiac valves, pericardial and myocardial fibrosis and accelerated atherosclerosis, most of which take from several years to decades to present (*3, 4*). The mechanisms by which radiation causes late cardiac injury are not yet fully understood.

We have previously shown that local heart irradiation in a rat model caused enhanced mitochondrial permeability transition pore (mPTP) opening within hours after irradiation and lasting for several months. Moreover, mitochondria isolated from irradiated hearts showed reduced *ex vivo* basal (state 2) respiration when tested in the presence of respiratory complex II substrate succinate combined with the complex I inhibitor rotenone. Respiration was not altered in the presence of complex I substrates glutamate and malate. Moreover, we showed that mitochondrial tetramethylrhodamine methyl ester (TMRM) uptake was reduced, indicative of reduced mitochondrial membrane potential, at time points up to two weeks after irradiation (*5*). The exact role of these mitochondrial changes in the pathophysiology of RIHD remains to be determined.

The natural vitamin E analogs, tocotrienols, have emerged as some of the strongest radiation protectors of all natural

Editor's note. The online version of this article (DOI: 10.1667/RR13915.1) contains supplementary information that is available to all authorized users.

[1] Address for correspondence: University of Arkansas for Medical Sciences, Division of Radiation Health, Department of Pharmaceutical Sciences, 4301 West Markham, Slot 522-10, Little Rock, AR 72205; e-mail: vmohanseenivasan@uams.edu.

compounds that have been tested so far (*6, 7*).[2] Moreover, tocotrienols have particular properties that may make them effective against cardiovascular disease. While tocotrienols have antioxidant properties as strong as α-tocopherol (*8*), they accumulate in endothelial cells to at least 30-fold higher levels than α-tocopherol and modulate at least 20-fold larger numbers of genes in endothelial cells (*9, 10*). Moreover, γ- and δ-tocotrienols reduce the intracellular levels of 3-hydroxy-3-methylglutaryl-coenzyme A (HMG-CoA) reductase, the rate-limiting enzyme in cholesterol biosynthesis (*11, 12*). Lastly, a recent study has shown that tocotrienols protect against oxidative stress-induced mitochondrial dysfunction (*13*). In the current study, we examined the effects of tocotrienols on radiation-induced mitochondrial changes and functional and structural manifestations of RIHD in our rat model of local heart irradiation.

All forms of vitamin E are fat soluble, which hampers their absorption in the gut upon oral administration. Tocomin SupraBio® (TSB) is a tocotrienol-enriched extract from palm oil that contains 17% tocotrienols (8% γ-tocotrienol, 5% α-tocotrienol, 3% δ-tocotrienol, 1% β-tocotrienol) and 5% α-tocopherol in a self-emulsifying delivery system designed for enhanced oral absorption (*14*). We have previously shown that oral administration of TSB in our rat model caused significant increases in plasma levels of all forms of vitamin E present in the TSB mixture (*15*). Tocotrienols and tocopherols may have anticancer activities and may also radiosensitize cancer cells (*16–18*). Nonetheless, administering any radiation protection compound before the onset of radiotherapy may not be preferable because of potential interactions with the effects of radiation on the tumor cells. However, since previous studies suggest that tocotrienols are most effective when administered 24 h before irradiation (*6, 19–21*), the main goal of this study was to first provide proof of principle by testing the effects of TSB when administered 24 h before irradiation.

MATERIALS AND METHODS

Animal Model and Administration of TSB

All procedures in this study were approved by the Institutional Animal Care and Use Committee of the University of Arkansas for Medical Sciences. Male Sprague-Dawley rats (Harlan® Laboratories Inc., Indianapolis, IN) were maintained in our Division of Laboratory Animal Medicine on a 12:12 light-dark schedule with free access to food and water. Upon reaching a weight of 250–290 g, the rats were administered 500 μl of TSB, translating to 230 mg tocotrienols/kg body weight or 500 μl vehicle (self-emulsifying formulation), via oral gavage 24 h before local heart irradiation. TSB and vehicle were kindly provided by Carotech BHD. (Perak, Malaysia).

Local Heart Irradiation

Rats received local heart irradiation with the Small Animal Conformal Radiation Therapy device (SACRTD) developed at our institution. The SACRTD consists of a 225 kVp X-ray source (GE Isovolt Titan 225, GE Sensing and Inspection Technologies, Billerica, MA) mounted on a custom-made ''gantry'', a stage mounted on a robotic arm positioning system (Viper™ s650, Adept Technology Inc., Pleasanton, CA), and a flat panel digital X-ray detector of 200 μm resolution (XRD 0820 CM3, PerkinElmer® Inc., Waltham, MA). For the purpose of local heart irradiation, a brass and aluminum collimating assembly was attached to the X-ray tube to produce a 19 mm diameter field at the isocenter (*22*).

Dosimetry was performed with a PinPoint® chamber (PTW N301013, PTW, Freiburg, Germany; ADCL calibrated for 225 kV) and Gafchromic® EBT-2 films (Ashland® Inc., Covington, KY) placed in a solid water phantom as previously described (*23*). For local heart irradiation, rats were anesthetized with 3% isoflurane and placed vertically in a cylindrical Plexiglas holder that was cut out to remove any Plexiglas material between the radiation beam and the chest. The heart was exposed in three 19 mm diameter fields (anterior-posterior and two lateral fields) of 7 Gy each (225 kV, 13 mA, 0.5 mm Cu filtration resulting in 1.92 Gy/min at 1 cm tissue depth). We previously showed that a cardiac dose of 21 Gy in Sprague-Dawley rats caused changes in left ventricular (LV) mitochondria, intracellular signaling molecules and moderate long-term changes in cardiac function and structure (*5, 15, 24*). The three doses of 7 Gy were given immediately after each other. Before each exposure the location of the heart was verified with the X-ray detector (70 kV, 5 mA, <1 cGy) and, if necessary, the position of the rat was adjusted with the use of the robotic arm. The cardiac targeting of the heart is shown in Supplementary Fig. S1 (http://dx.doi.org/10.1667/RR13915.1.S1) and has been previously described by our group (*22*).

Rats were sacrificed at 2 and 28 weeks after local heart irradiation, and the hearts were collected for analysis. The 2 week time point consisted of four experimental groups: sham-irradiated vehicle-pretreated, sham-irradiated TSB-pretreated, irradiated vehicle-pretreated and irradiated TSB-pretreated (5 animals per group). The 28 week time point consisted of three experimental groups: sham-irradiated vehicle-pretreated, irradiated vehicle-pretreated and irradiated TSB-pretreated (9–10 animals per group).

Echocardiography

Echocardiography (ECGs) was performed as described previously (*25*), using a Vevo® 2100 imaging system (VisualSonics Inc., Toronto, Canada) with the MS250 transducer (13–24 MHz). Animals were anesthetized with 1.5–2% isoflurane and hair was removed from the chest with clippers followed by a depilatory cream. The rats were placed on a warmed platform that recorded ECGs from the paws. ECGs were used to detect bradycardia (heart rate <250 bpm) and arrhythmia. Short axis M-mode recordings at the mid-LV level were used to obtain LV anterior wall (LVAW), posterior wall (LVPW), inner diameter (LVID), ejection fraction (EF), fractional shortening (FS), stroke volume, cardiac output and heart rate.

High-Performance Liquid Chromatography Quantification of Glutathione

High-performance liquid chromatography with electrochemical detection (HPLC-ECD) was used to evaluate levels of reduced glutathione (GSH) and oxidized glutathione (GSSG). Details of this method have been previously described (*26*). In short, approximately 50 mg of tissue was minced and homogenized in 500 μl of ice-cold phosphate buffered saline. To precipitate proteins, 150 μl of 10%

[2] Fu. Q., Berbee, M., Boerma, M., Wang, J., Kumar, K. S., Hauer-Jensen, M. The vitamin E analog, gamma-tocotrienol, protects against tissue injury and lethality after total body irradiation partly via inhibition of HMG-CoA reductase (Abstract). Presented at the Fifty-Fourth Annual Meeting of the Radiation Research Society, Boston, MA, 2008.

metaphosphoric acid was added to 100 µl of tissue homogenate and incubated for 30 min on ice. The samples were then centrifuged at 18,000*g* at 4°C for 15 min, and 20 µl of the resulting supernatants were injected into the HPLC column for metabolite quantification, while the pellet underwent protein analysis using a BCA protein assay (Sigma-Aldrich® LLC, St. Louis, MO). Free protein-unbound GSH and GSSG were separated by HPLC-ECD coupled with a solvent delivery system (model no. 580E, ESA Inc., Chelmsford, MA). A reverse phase C_{18} Shisheido column (3 µ; 4.6 × 150 mm) was obtained from Phenomenex® Inc. (Torrance, CA). Isocratic elution with a mobile phase consisting of 50 m*M* sodium phosphate monobasic, monohydrate, 1.0 m*M* ion-pairing reagent OSA, 4% acetonitrile (v/v), adjusted to pH 2.7 with 85% phosphoric acid, was performed at ambient temperature at a flow rate of 1.0 mL/min and a pressure of 120–140 kgf/cm^2 (1,800–2,100 psi). Tissue homogenates were directly injected onto the column using an ESA Autosampler (model no. 507E). The results are expressed as n*M* per mg total protein.

Ex Vivo Analysis of Mitochondria

Mitochondrial respiration, mPTP opening and measurement of mitochondrial membrane potential were performed as described before (*5*). In short, rats were anesthetized with 3% isoflurane, the heart was isolated, and 180–200 mg of LV tissue was immediately minced and homogenized in 10 mL of a 10 m*M* HEPES buffer containing 225 m*M* mannitol, 75 m*M* sucrose, 1 m*M* EGTA and 0.5% (w/v) fatty acid-free BSA (pH 7.4) using a mechanical Dounce homogenizer with a Teflon pestle. The homogenate was centrifuged at 700*g* for 10 min at 4°C, and the supernatant collected and centrifuged at 12,500*g* for 30 min to obtain the mitochondrial pellet. Mitochondria were used immediately to measure mitochondrial respiration, mPTP opening and mitochondrial membrane potential, as described previously (*5*).

Mitochondrial respiration was analyzed with an XF96 Extracellular Flux Analyzer (Seahorse Bioscience, North Billerica, MA). Mitochondria were placed in an XF96 microplate, 10 or 15 µg mitochondrial mass per well (8 wells for each), and mixed with 10 m*M* succinic acid and 0.2 µ*M* rotenone. The plates were centrifuged at 4°C, 2,000*g* for 20 min to attach the mitochondria to the bottom of the wells, then incubated at 37°C for 10 min and transferred to the XF96 Extracellular Flux Analyzer. Four baseline measurements were acquired, followed by readings after sequential addition of ADP (4 µ*M*), oligomycin (4 µ*M*), p-trifluoromethoxyphenylhydrazone (FCCP) (4 µ*M*) and antimycin A (10 µ*M*). The oxygen consumption rate (OCR) was calculated with XF96 software. Each XF96 plate contained mitochondria from one heart of each experimental group, and within each plate the OCR of the irradiated mitochondria was calculated relative to the OCR of the sham-irradiated mitochondria.

To assess mPTP opening, mitochondria were washed in 10 m*M* HEPES buffer containing 395 m*M* sucrose and 0.1 m*M* EGTA to remove excess BSA. MPTP opening was then assessed in a swelling assay, in which mitochondria were resuspended in swelling buffer containing 120 m*M* KCl, 10 m*M* Tris HCl, and 5 m*M* KH_2PO_4 and exposed to vehicle, 250 µ*M* $CaCl_2$ or 250 µ*M* $CaCl_2$ in combination with 2 µ*M* cyclosporin A (CsA), as an inhibitor of transition pore opening. In another set of experiments mPTP opening was assessed by adding either 5 µ*M* doxorubicin or 5 µ*M* doxorubicin combined with 2 µ*M* CsA. MPTP opening in response to $CaCl_2$ or doxorubicin will lead to mitochondrial swelling, which is detected by a reduction in optical density at 540 nm (OD540nm). Optical density at 540 nm was measured with a Synergy™ 4 microplate reader (BioTek®, Winooski, VT), immediately before the assay and every 2 min thereafter for a total of 20 min.

Mitochondrial membrane potential was assessed with TMRM, a cationic dye that accumulates in mitochondria in proportion to the mitochondrial membrane potential. Mitochondria were resuspended in 10 m*M* HEPES containing 395 m*M* sucrose and 0.1 m*M* EGTA, loaded with 50 nm or 200 nm TMRM and incubated at room temperature for 15 min. Mitochondria were centrifuged at 14,000 rpm for 3 min to remove excess TMRM, and the fluorescence intensity of the mitochondrial pellets was determined at 590 nm in a Synergy 4 microplate reader (BioTek) and normalized to mitochondrial protein content as measured with a BCA protein assay. Each isolation of mitochondria included one heart from each experimental group, and the normalized TMRM signals were calculated relative to the TMRM signal of the mitochondria from the sham-irradiated heart.

Western Blots

Western blots were performed as previously described (*15, 27*). In short, LV tissue was homogenized in RIPA buffer with inhibitor cocktails of proteases (10 µL/mL) and phosphatases (10 µL/mL, both Sigma-Aldrich), centrifuged at 20,000*g* at 4°C for 15 min, and the supernatant was collected. Similarly, mitochondria pellets were lysed with RIPA buffer containing protease and phosphatase inhibitors for 30 min with intermittent vortexing, followed by sonication for 6 s. The lysates were centrifuged at 14,000 rpm for 10 min and the supernatants were collected. Amounts of protein were determined with a BCA protein assay. A total of 50 µg protein was prepared in Laemmli sample buffer containing β-mercaptoethanol (1:20 vol/vol) and boiled for 2–3 min. Protein samples were separated in 4–20% TGX™ Mini-PROTEAN® polyacrylamide gels and transferred to PVDF membranes (Bio-Rad Laboratories Inc., Hercules, CA).

Nonspecific antibody binding was reduced by TSB containing 0.05% Tween-20 and 5% nonfat dry milk. Membranes were then incubated overnight with rabbit anti-Bax, rabbit anti-Bcl2 (Santa Cruz Biotechnology® Inc., Dallas, TX) or rabbit anti-caspase 3 (Cell Signaling Technology®, Danvers, MA) both in TSB containing 5% nonfat dry milk and 0.1% Tween-20, followed by HRP conjugated mouse anti-rabbit (Cell Signaling Technology) or HRP-conjugated goat anti-mouse (Jackson ImmunoResearch Laboratories Inc., West Grove, PA). Protein loading was corrected by incubating membranes in mouse anti-GAPDH for whole tissue lysates (Santa Cruz Biotechnology, Inc.) or mouse anti-F0-F1 ATPase for mitochondrial lysates (Life Technologies, Grand Island, NY), followed by HRP-conjugated goat anti-mouse. Antibody binding was visualized with ECL™ Plus Western Blotting Detection reagent (GE Healthcare Bio-Sciences, Pittsburgh, PA) on CL-Xposure Film (Thermo Fisher Scientific, Boston MA). Films were scanned using an AlphaImager® gel documentation system (ProteinSimple®, San Jose, CA) and protein bands were quantified with the public domain software ImageJ (National Institutes of Health, Bethesda, MD).

Histology

Hearts were fixed in 37% formaldehyde and embedded in paraffin. Histology and immunohistochemistry were performed as previously described (*27*). In short, for determination of collagen deposition and areas of myocardial degeneration, sections were deparaffinized, rehydrated and incubated in Sirius Red (American Master*Tech Scientific Inc., Lodi, CA) supplemented with Fast Green (Fisher Scientific™, Thermo Fisher Scientific Inc.). The sections were scanned with an Aperio™ ScanScope® CS2 slide scanner and analyzed with Aperio ImageScope 12 software (both scanner and software from Leica Biosystems Imaging Inc., Nussloch, Germany) to determine the percentage tissue area positive for collagens.

To visualize mast cells, deparaffinized and rehydrated sections were incubated in 0.5% toluidine blue in 0.5 *N* HCl for 72 h, followed by 0.7 *N* HCl for 10 min. Mast cells were counted using an Axioskop transmitted light microscope (Carl Zeiss, Jena, Germany).

A lectin staining was used to determine microvascular density. Sections were deparaffinated and rehydrated, and antigen retrieval was performed by treating the sections with 10 m*M* sodium citrate (pH 6.0) at 95°C for 20 min. Sections were allowed to cool down prior to incubation in 1% H_2O_2 in methanol for 30 min to quench the endogenous peroxidase activity. Sections where then incubated with

biotinylated Lycopersicon esculentum (tomato) lectin (1:200, Vector Laboratories, Burlingame, CA) for 90 min at room temperature. Lectin staining was visualized by incubating the sections in avidin-biotin-peroxidase complex (Vector Laboratories) for 45 min at room temperature and then in 0.5 mg/ml DAB (Sigma-Aldrich) and 0.003% H_2O_2 for 5 min. After counterstaining with hematoxylin, sections were dehydrated and mounted. Sections were then scanned with an Aperio ScanScope CS2 slide scanner and analyzed with Aperio ImageScope 12 software. Four fields were randomly selected to count the lectin-stained capillaries, and the total number of capillaries was divided by the area of the field to obtain capillary density. The average value of capillary density of each section was used as a single data point for statistical analysis.

Statistical Analysis

Data are shown as averages ± standard error of the mean (SEM). Data were evaluated with two-way analysis of variance (ANOVA) or repeated measures ANOVA (mitochondrial swelling assay), followed by Newman-Keuls individual comparisons, using the NCSS 8 software package (NCSS, Kaysville, UT). The criterion for significance was $P < 0.05$.

RESULTS

Heart and Body Weights

There were no significant differences in heart or body weights between any of the groups at both time points (data not shown).

LV Tissue GSH and GSSG Levels

We first determined GSH and GSSG levels in LV tissues obtained in our previous experiments at time points from 2 h until 9 months after local heart irradiation (21 Gy single dose) in male Sprague-Dawley rats. A significant increase in GSSG levels caused a significant decrease in GSH/GSSG ratios in LV tissues at time points from 2 h to 10 weeks after local heart irradiation, indicative of prolonged oxidative stress (Supplementary Fig. S2; http://dx.doi.org/10.1667/RR13915.1.S1). Because all natural forms of vitamin E are strong antioxidants, we determined the effects of TSB pretreatment on LV GSH/GSSG. Local heart irradiation caused a small but significant reduction in GSH/GSSG at 2 and 28 weeks, while the GSH/GSSG ratios in the TSB-pretreated irradiated groups were not significantly different from the controls (Fig. 1).

LV Tissue and Mitochondrial Protein Levels of Bax and Bcl2

Radiation caused a significant increase in the total LV expression of Bax at the 2 week time point and elevated Bax/Bcl2 ratios at both 2 and 28 weeks (Fig. 2A). Increased LV Bax/Bcl2 ratios coincided with significant increases in mitochondrial Bax/Bcl2 ratios at both time points (Fig. 2B). LV tissue and mitochondrial Bax/Bcl2 ratios in the TSB-pretreated groups were not significantly different from vehicle-pretreated sham controls (Fig. 2).

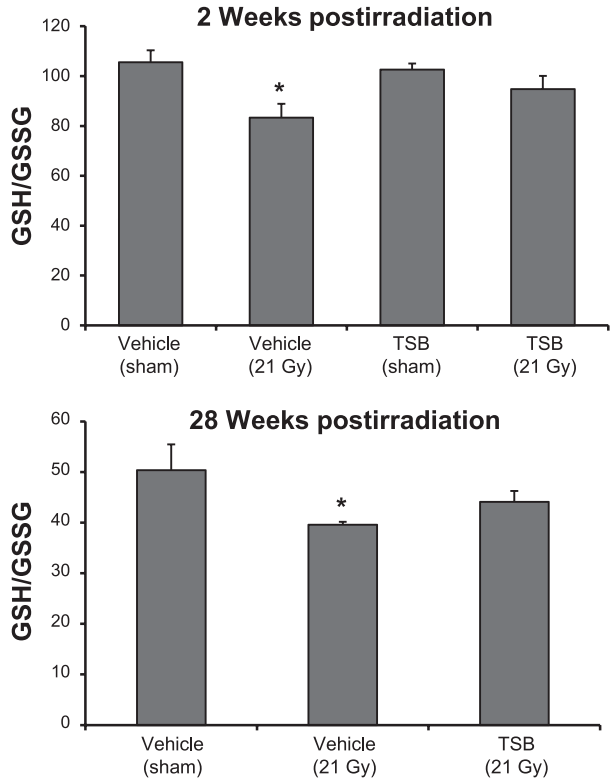

FIG. 1. Effects of radiation and TSB on LV GSH/GSSG ratios. TSB pretreatment maintained GSH/GSSG ratios in LV tissues at 2 weeks and 28 weeks after irradiation. Average ± SEM, n = 5–6. *$P <$ 0.05 compared to sham-irradiated control.

Mitochondrial Susceptibility to mPTP Opening and Changes in Mitochondrial Membrane Potential

Mitochondria isolated at 2 and 28 weeks postirradiation showed increased swelling in response to *ex vivo* stimulation with $CaCl_2$ (Fig. 3A) and doxorubicin (Supplementary Fig. S3; http://dx.doi.org/10.1667/RR13915.1.S1). Mitochondrial swelling was inhibited by CsA, confirming that it was due to mPTP opening. Moreover, reduced TMRM uptake indicated a reduced mitochondrial membrane potential at 2 weeks (Supplementary Fig. S3; http://dx.doi.org/10.1667/RR13915.1.S1). TSB pretreatment prevented calcium- and doxorubicin-induced mitochondrial swelling and maintained the mitochondrial membrane potential (Fig. 3 and Supplementary Fig. S3; http://dx.doi.org/10.1667/RR13915.1.S1).

Mitochondrial Respiration

In agreement with the results from our previous work, we observed a reduction in state 2 respiration in mitochondria isolated at 2 weeks after irradiation and *ex vivo* analyzed in succinate-rotenone. TSB pretreatment protected against these radiation-induced changes (Fig. 4A). No alterations were observed in mitochondrial respiration at 28 weeks after irradiation (Fig. 4B). Lastly, as in our previous studies, mitochondrial respiration was not altered when glutamate-

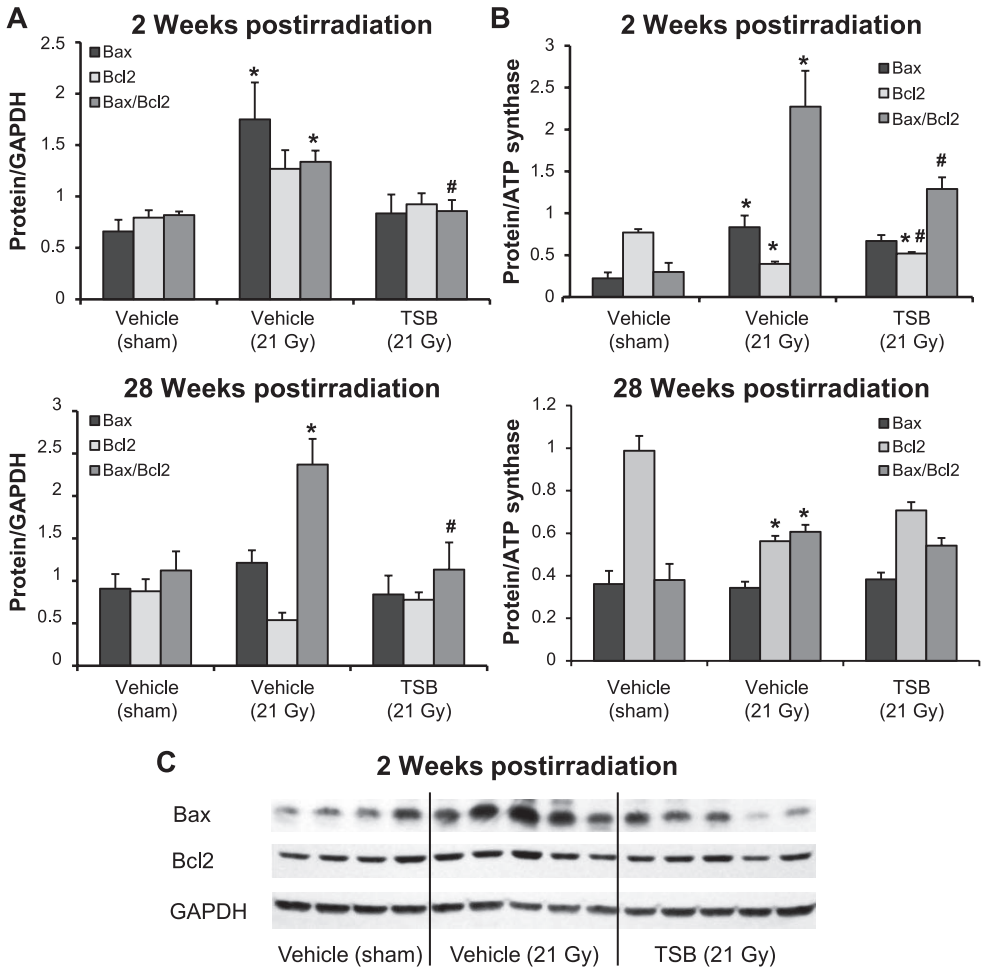

FIG. 2. Effects of TSB on whole tissue and mitochondrial protein levels of Bax and Bcl2. Local heart irradiation caused an increase in LV Bax levels at 2 weeks and an increase in Bax/Bcl2 ratios at both 2 and 28 weeks (panel A). Mitochondrial Bax/Bcl2 ratios were increased at 2 and 28 weeks after irradiation (panel B). LV tissue and mitochondrial Bax/Bcl2 ratios in the TSB-pretreated groups were not significantly different from vehicle-pretreated sham controls. Average ± SEM, n = 5–6. *$P < 0.05$ compared to sham-irradiated control. #$P < 0.05$ compared to vehicle-pretreated irradiated. Panel C: Representative Western blot image of Bax and Bcl2 at 2 weeks postirradiation.

malate was provided as substrates of complex I (data not shown).

LV Protein Levels of Cleaved Caspase 3

Increased Bax/Bcl2 ratios and mitochondrial membrane modifications may lead to induction of cleaved caspase 3. We observed a significant increase in cleaved caspase 3 at 2 and 28 weeks after irradiation. TSB pretreatment significantly reduced cleaved caspase 3 protein levels at both time points (Supplementary Fig. S4; http://dx.doi.org/10.1667/RR13915.1.S1).

Ultrasound Parameters and Cardiac Remodeling

Because radiation-induced functional and histopathological changes are delayed effects of X irradiation, we performed ultrasound and histological analysis at the 28 week time point (Table 1). Seven out of 10 irradiated animals showed bradycardia (heart rate <250 bpm when under 1.5–2% isoflurane). Moreover, radiation caused a significant increase in total cardiac diameter, LVID and volume in diastole. Lastly, although irradiated hearts showed an increased stroke volume, irradiated hearts could not maintain cardiac output due to the reduced heart rate. None of the parameters were significantly modified by TSB (Table 1). In addition, TSB pretreatment enhanced the number of cardiac mast cells, but did not prevent radiation-induced cardiac fibrosis or reduced LV capillary density (Fig. 5 and Supplementary Fig. S5; http://dx.doi.org/10.1667/RR13915.1.S1).

DISCUSSION

In this study we tested the effects of a single oral dose of the tocotrienol-enriched formulation TSB on cardiac functional, histological and mitochondrial alterations at an

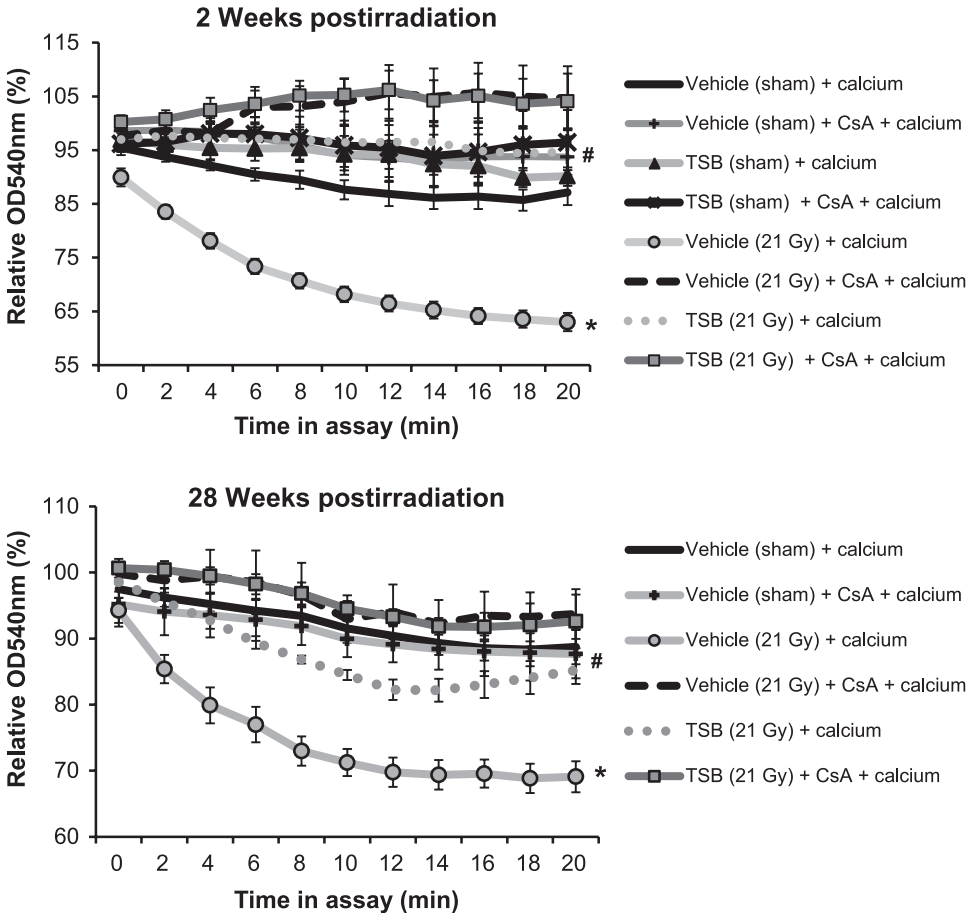

FIG. 3. Effects of TSB pretreatment on radiation-induced mitochondrial susceptibility to mPTP opening. Susceptibility to mPTP opening in isolated mitochondria is examined by mitochondrial swelling, indicated by a reduction in the optical density at 540 nm (OD540nm) in response to $CaCl_2$. The OD540nm of mitochondria in the swelling assay is expressed relative to the OD540nm of the same sample immediately before the start of the assay. Mitochondria are *ex vivo* exposed to the mPTP inhibitor CsA to confirm that swelling is due to mPTP opening. *In vivo* TSB pretreatment prevented mPTP opening in response to $CaCl_2$ in mitochondria isolated at both 2 and 28 weeks after local heart irradiation. Average ± SEM, n = 5. $^{*}P < 0.05$ compared to sham-irradiated control. $^{\#}P < 0.05$ compared to vehicle-pretreated irradiated.

early and late time point after local heart irradiation. While radiation-induced mitochondrial changes were prevented by TSB, no improvements were observed in cardiac function or histological parameters.

For this study, a single dose of radiation was examined. Therapeutic radiation is typically fractionated at 2 Gy per fraction. The effects of TSB treatment prior to fractionated irradiation remain to be determined.

It is well known that exposure to radiation results in the formation of reactive oxygen species (ROS) that cause oxidative damage of DNA, protein and lipids (*28, 29*). This may lead to metabolic oxidative stress that contributes to the biological effects of radiation long after the time of exposure (*30*). Glutathione plays an important role against radiation-induced oxidative damage (*31*), and the ratio of reduced to oxidized glutathione serves as an index of the redox status of the cell. Because all natural forms of vitamin E are strong antioxidants, and reducing oxidative stress may therefore be one of the mechanisms by which TSB protects against mitochondrial changes, we examined the effects of TSB on the redox status of LV tissues after irradiation. First, we examined GSH/GSSG ratios in LV tissues obtained from a previous time-course study (*5*). Radiation caused a prolonged and significant decrease in the GSH/GSSH ratios from 2 h to 10 weeks after irradiation, demonstrating prolonged radiation-induced oxidative stress in the heart. In TSB-pretreated hearts GSH/GSSG ratios were not significantly different from their sham counterparts. Although the differences between experimental groups were subtle, the results may suggest a long-term improvement in redox status with TSB pretreatment.

Under conditions of stress, levels of the pro-apoptotic Bax protein are increased relative to the anti-apoptotic Bcl2, and Bax is translocated to the outer mitochondrial membrane (*32–35*). Consistent with our previous studies (*5*), our current study shows the radiation-induced increases in Bax and Bax/Bcl2 ratios in total left ventricular protein lysates and in mitochondrial lysates. A single-dose administration

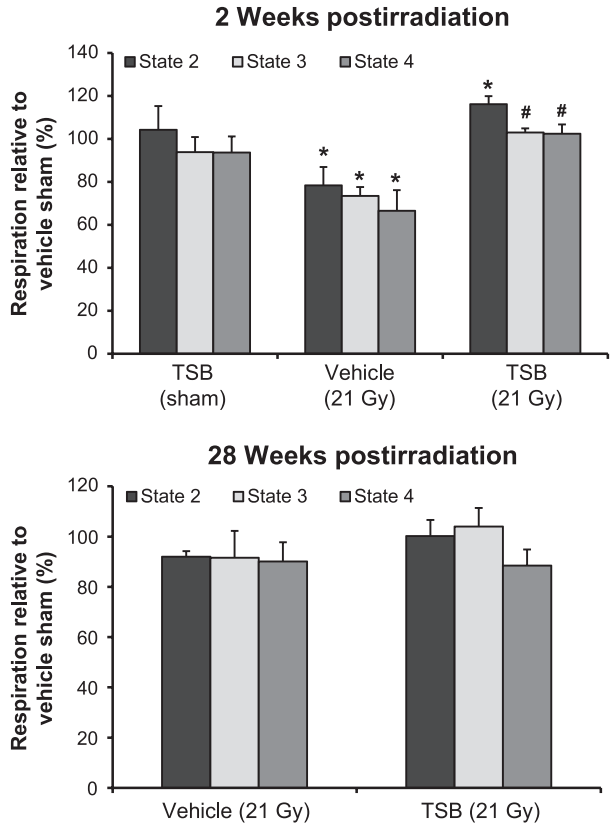

FIG. 4. Effects of TSB pretreatment on radiation-induced changes in mitochondrial respiration. The graphs show *ex vivo* oxygen consumption in the presence of succinate and rotenone at 2 and 28 weeks after irradiation, relative to oxygen consumption in mitochondria isolated from vehicle-pretreated sham-irradiated animals. TSB pretreatment protected against a radiation-induced decline in respiration at 2 weeks. Mitochondrial respiration did not show any significant changes at 28 weeks after irradiation. Average ± SEM, n = 5. *$P < 0.05$ compared to sham-irradiated control. #$P < 0.05$ compared to vehicle-pretreated irradiated.

TABLE 1
Echocardiography Parameters Measured at 28 Weeks after Local Heart Irradiation

	Vehicle (sham)	Vehicle (21 Gy)	TSB (21 Gy)
LVAW, systole (mm)	3.2 ± 0.1	3.3 ± 0.1	3.2 ± 0.1
LVAW, diastole (mm)	2.2 ± 0.1	1.9 ± 0.1	2.2 ± 0.2
LVID, systole (mm)	5.0 ± 0.2	5.2 ± 0.2	5.4 ± 0.3
LVID, diastole (mm)	8.3 ± 0.2	9.5 ± 0.3*	9.4 ± 0.4
LVPW, systole (mm)	3.1 ± 0.1	3.2 ± 0.1	3.1 ± 0.1
LVPW, diastole (mm)	2.1 ± 0.1	2.0 ± 0.1	2.0 ± 0.1
Diameter, systole (mm)	4.7 ± 0.2	5.3 ± 0.3	5.5 ± 0.3
Diameter, diastole (mm)	8.4 ± 0.2	9.8 ± 0.3*	9.5 ± 0.4
Volume, systole (μl)	106 ±12	138 ± 18	151 ± 19
Volume, diastole (μl)	388 ± 23	542 ± 36*	517 ±53
Ejection fraction (%)	73 ± 2	75 ± 3	71 ± 3
Fractional shortening (%)	44 ± 2	46 ± 2	43 ± 3
Stroke volume (μl)	282 ± 14	403 ± 41*	367 ± 40
Cardiac output (ml/min)	92 ± 5	72 ± 6*	71 ± 8
Heart rate (bpm)	327 ± 9	197 ± 29*	206 ± 26*
Number of animals with bradycardia (heart rate < 250 bpm)	0/9	7/10	7/9

Notes. High-resolution small animal ultrasound was used to determine cardiac function. Average ± SEM, n = 9–10.
* $P < 0.05$ compared to sham-irradiated control.

of TSB 24 h before irradiation was effective in maintaining Bax/Bcl2 ratios at control levels. A recently published study also demonstrated the ability of γ-tocotrienol to preserve the protein expression of Bax and decrease Bax/Bcl2 ratios in skin fibroblasts subjected to oxidative stress (*36*). Insertion of Bax into the mitochondrial membrane is associated with increased mitochondrial membrane permeability and loss of membrane potential (*37*). As described previously (*5*), a reduction in mitochondrial membrane potential was observed only at 2 weeks after irradiation. TSB pretreatment preserved the membrane potential in irradiated mitochondria.

Impaired mitochondrial function and altered Bax/Bcl2 ratios may eventually lead to activation of caspases and cellular apoptosis. We found that TSB pretreatment protected against radiation-induced increases in cleaved caspase 3 in the heart. Nonetheless, we have previously shown that local heart irradiation in our rat model does not lead to significant increases in the number of apoptotic cells (*5*), and we therefore believe that apoptosis may not play a significant role in the development of cardiac radiation injury in our model.

Mitochondrial permeability transition (MPT) is characterized by a loss of mitochondrial membrane potential, and mPTP opening in response to stimuli such as calcium, inorganic phosphate or ROS to induce mPTP opening (*38–40*). We studied the opening of mPTP with a mitochondrial swelling assay. In accordance with our previous work, mitochondria isolated from irradiated hearts showed pronounced mitochondrial swelling in response to exogenous calcium. Here we also examined the effects of doxorubicin, a chemotherapeutic agent commonly used in combination with radiotherapy. Doxorubicin has profound cardiotoxic side effects that may be synergistic with radiation (*41*). Although doxorubicin's cardiotoxicity is due in part to mitochondrial dysfunction (*42*), previous studies have shown that under *in vivo* conditions doxorubicin alone did not induce mPTP opening (*43*). Similarly, doxorubicin did not induce swelling in mitochondria isolated from sham-irradiated hearts in our study. On the other hand, mitochondria isolated from irradiated hearts did show significant doxorubicin-induced mPTP opening, suggesting that previous exposure to ionizing radiation made these mitochondria more susceptible to the effects of doxorubicin.

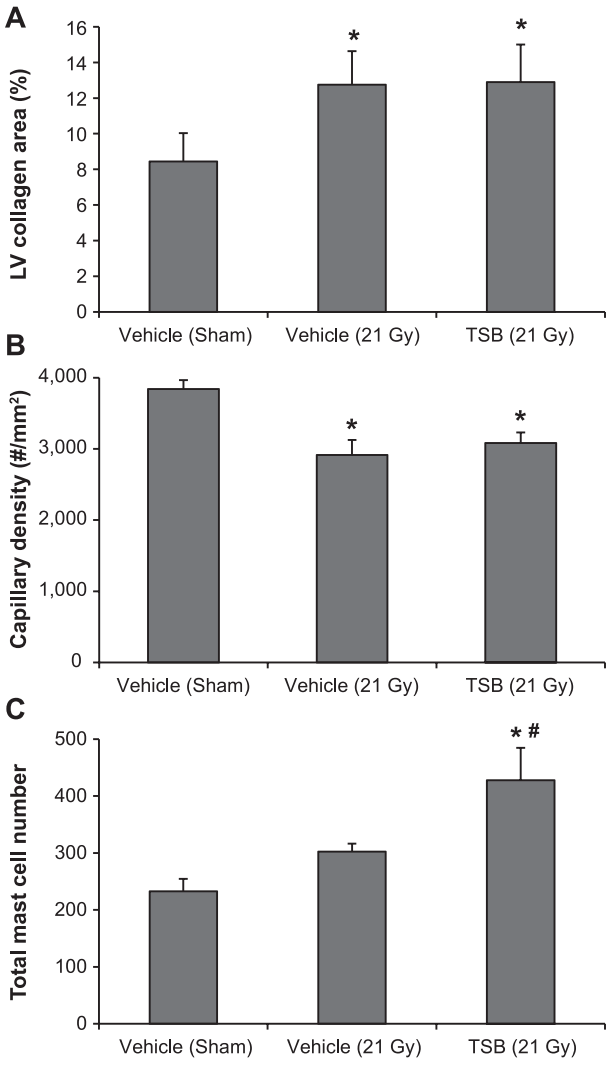

FIG. 5. Effects of TSB on cardiac remodeling at 28 weeks after irradiation. TSB did not modify a radiation-induced increase in LV collagen deposition (panel A) or decrease in capillary density (panel B). While radiation alone had no significant effect on cardiac mast cell numbers, TSB pretreatment significantly enhanced mast cell numbers in irradiated hearts (panel C). Average ± SEM, n = 9–10. $^{*}P < 0.05$ when compared to sham-irradiated control. $^{\#}P < 0.05$ compared to vehicle-pretreated irradiated.

Interestingly, a recent study showed that γ-tocotrienol inhibited MPT and blocked mitochondrial membrane depolarization in oxidant-induced injury in renal proximal tubular cells (*44*). TSB pretreatment prevented mPTP opening in response to both calcium and doxorubicin. These observations suggest that TSB may serve as an effective candidate to prevent mPTP opening in mitochondria induced by secondary stressors in the irradiated heart.

Previous studies have shown prolonged alterations in mitochondrial respiration in animal models of local heart irradiation. Barjaktarovic *et al*. reported decreased succinate-dependent respiration (state 2) with unaltered state 3 respiration in LV tissues of mouse hearts at 4 and 40 weeks after irradiation (*45, 47*). Franken *et al*. have shown significant reduction in state 3 respiration at 8 weeks after local heart irradiation in the rat with succinate and β-hydroxybutyrate as *ex vivo* substrates (*46*). In our approach, we examined oxygen flux in isolated mitochondria. We previously demonstrated reduced state 2 and state 4 respiration through complex II (succinate-dependent) with no alterations in respiration through complex I at 2 weeks after irradiation (*5*). In the current study, a single oral dose of TSB administered 24 h before irradiation significantly preserved the respiratory capacity in succinate-driven respiration at 2 weeks. Similarly, γ-tocotrienol improves the state 3 respiration and function of the electron transport chain upon oxidant injury in primary cell cultures (*44*).

We next studied whether TSB had effects on late cardiac function and remodeling. The rodent heart has a strong ability to compensate for myocardial structural damage to maintain cardiac output (*48*). Nonetheless, in our experiment, due to a significantly reduced heart rate, cardiac output was not maintained despite a significant increase in stroke volume. A single oral dose of TSB 24 h before irradiation was not successful in preventing cardiac functional alterations. Adverse myocardial remodeling is a common manifestation of RIHD and coincides with increased cardiac mast cell numbers (*49*). TSB did not protect against radiation-induced decrease in capillary density or collagen deposition and enhanced cardiac mast cell numbers.

Amifostine is currently the only approved radiation protector in radiation therapy, although it is not generally used because of its side effects. Amifostine was previously tested in rat models of local heart irradiation (*50, 51*). Amifostine protected against radiation-induced myocardial degeneration (*50*) and cardiac function loss (*51*), and was thereby more effective than the TSB administration in our model. While the effects of amifostine on cardiac fibrosis were small, macroscopic radiation injury in the lung was significantly reduced (*51*). Therefore, it cannot be excluded that amifostine was protective by modifying heart–lung interactions (*52*). However, in our model we do not administer a large enough dose of radiation to the lung to induce significant pulmonary inflammation or fibrosis.

From our studies it may be concluded that TSB pretreatment inhibited radiation-induced mitochondrial changes in the heart, including susceptibility to mPTP opening, reduced mitochondrial membrane potential, and reduced mitochondrial respiration as measured with *ex vivo* succinate-rotenone as the substrate. However, TSB pretreatment did not prevent radiation-induced long-term alterations in cardiac function and adverse cardiac remodeling. These findings suggest that changes in mitochondrial properties, as measured in this study, are not the main underlying mechanism of radiation toxicity in the heart. Repeated administration of tocotrienols may be more effective in reducing late manifestations of RIHD, by modifying additional contributing factors such as endothelial dysfunction.

SUPPLEMENTARY INFORMATION

Fig. S1. Image-guided irradiation of the rat heart.

Fig. S2. HPLC analysis of reduced glutathione (GSH) and oxidized glutathione (GSSG) in left ventricles at 2 h to 9 months after local heart irradiation in adult male Sprague-Dawley rats.

Fig. S3. Effects of radiation and TSB on mitochondrial membrane properties.

Fig. S4. Effects of radiation and TSB on protein levels of cleaved caspase 3.

Fig. S5. Representative images of histological staining at 28 weeks after irradiation.

ACKNOWLEDGMENTS

This work was supported by the National Institutes of Health (CA148679, CA71382) and the American Cancer Society (RSG-10-125-01-CCE).

Received: September 17, 2014; accepted: December 4, 2014; published online: February 24, 2015

REFERENCES

1. Gatta G, Zigon G, Capocaccia R, Coebergh JW, Desandes E, Kaatsch P, et al. Survival of European children and young adults with cancer diagnosed 1995–2002. Eur J Cancer 2009; 45:992–1005.
2. Verdecchia A, Guzzinati S, Francisci S, De AR, Bray F, Allemani C, et al. Survival trends in European cancer patients diagnosed from 1988 to 1999. Eur J Cancer 2009; 45:1042–66.
3. Adams MJ, Hardenbergh PH, Constine LS, Lipshultz SE. Radiation-associated cardiovascular disease. Crit Rev Oncol Hematol 2003; 45:55–75.
4. Heidenreich PA, Hancock SL, Vagelos RH, Lee BK, Schnittger I. Diastolic dysfunction after mediastinal irradiation. Am Heart J 2005; 150:977–82.
5. Sridharan V, Aykin-Burns N, Tripathi P, Krager KJ, Sharma SK, Moros EG, et al. Radiation-induced alterations in mitochondria of the rat heart. Radiat Res 2014; 181:324–34.
6. Singh VK, Shafran RL, Jackson WE, III, Seed TM, Kumar KS. Induction of cytokines by radioprotective tocopherol analogs. Exp Mol Pathol 2006; 81:55–61.
7. Satyamitra MM, Kulkarni S, Ghosh SP, Mullaney CP, Condliffe D, Srinivasan V. Hematopoietic recovery and amelioration of radiation-induced lethality by the vitamin E isoform delta-tocotrienol. Radiat Res 2011; 175:736–45.
8. Yoshida Y, Niki E, Noguchi N. Comparative study on the action of tocopherols and tocotrienols as antioxidant: chemical and physical effects. Chem Phys Lipids 2003; 123:63–75.
9. Berbee M, Fu Q, Boerma M, Sree KK, Loose DS, Hauer-Jensen M. Mechanisms underlying the radioprotective properties of gamma-tocotrienol: comparative gene expression profiling in tocol-treated endothelial cells. Genes Nutr 2012; 7:75–81.
10. Naito Y, Shimozawa M, Kuroda M, Nakabe N, Manabe H, Katada K, et al. Tocotrienols reduce 25-hydroxycholesterol-induced monocyte-endothelial cell interaction by inhibiting the surface expression of adhesion molecules. Atherosclerosis 2005; 180:19–25.
11. Parker RA, Pearce BC, Clark RW, Gordon DA, Wright JJ. Tocotrienols regulate cholesterol production in mammalian cells by post-transcriptional suppression of 3-hydroxy-3-methylglutaryl-coenzyme A reductase. J Biol Chem 1993; 268:11230–8.
12. Song BL, Bose-Boyd RA. Insig-dependent ubiquitination and degradation of 3-hydroxy-3-methylglutaryl coenzyme a reductase stimulated by delta- and gamma-tocotrienols. J Biol Chem 2006; 281:25054–61.
13. Nowak G, Bakajsova D, Hayes C, Hauer-Jensen M, Compadre CM. gamma-Tocotrienol protects against mitochondrial dysfunction and renal cell death. J Pharmacol Exp Ther 2012; 340:330–8.
14. Sen CK, Khanna S, Roy S. Tocotrienols in health and disease: the other half of the natural vitamin E family. Mol Aspects Med 2007; 28:692–728.
15. Sridharan V, Tripathi P, Sharma S, Corry PM, Moros EG, Singh A, et al. Effects of late administration of pentoxifylline and tocotrienols in an image-guided rat model of localized heart irradiation. PLoS One 2013; 8:e68762.
16. Tran AT, Ramalinga M, Kedir H, Clarke R, Kumar D. Autophagy inhibitor 3-methyladenine potentiates apoptosis induced by dietary tocotrienols in breast cancer cells. Eur J Nutr 2014 (DOI: 10.1007/s00394-014-0707-y).
17. Srivastava JK, Gupta S. Tocotrienol-rich fraction of palm oil induces cell cycle arrest and apoptosis selectively in human prostate cancer cells. Biochem Biophys Res Commun 2006; 346:447–53.
18. Girdhani S, Bhosle SM, Thulsidas SA, Kumar A, Mishra KP. Potential of radiosensitizing agents in cancer chemo-radiotherapy. J Cancer Res Ther 2005; 1:129–31.
19. Berbee M, Fu Q, Boerma M, Wang J, Kumar KS, Hauer-Jensen M. gamma-Tocotrienol ameliorates intestinal radiation injury and reduces vascular oxidative stress after total-body irradiation by an HMG-CoA reductase-dependent mechanism. Radiat Res 2009; 171:596–605.
20. Berbee M, Fu Q, Garg S, Kulkarni S, Kumar KS, Hauer-Jensen M. Pentoxifylline enhances the radioprotective properties of gamma-tocotrienol: differential effects on the hematopoietic, gastrointestinal and vascular systems. Radiat Res 2010; 175:297–306.
21. Ghosh SP, Kulkarni S, Hieber K, Toles R, Romanyukha L, Kao TC, et al. Gamma-tocotrienol, a tocol antioxidant as a potent radioprotector. Int J Radiat Biol 2009; 85:598–606.
22. Sharma S, Moros EG, Boerma M, Sridharan V, Han EY, Clarkson R, et al. A novel technique for image-guided local heart irradiation in the rat. TCRT Express 2013; 1:47–57.
23. Sridharan V, Tripathi P, Sharma SK, Moros EG, Corry P, Lieblong BJ, et al. Cardiac inflammation after local irradiation is influenced by the kallikrein-kinin system. Cancer Res 2012; 72:4984–92.
24. Sridharan V, Sharma SK, Moros EG, Corry PM, Tripathi P, Lieblong BJ, et al. Effects of radiation on the epidermal growth factor receptor pathway in the heart. Int J Radiat Biol 2013; 89:539–47.
25. Sridharan V, Tripathi P, Sharma SK, Moros EG, Corry P, Lieblong BJ, et al. Cardiac inflammation after local irradiation is influenced by the kallikrein-kinin system. Cancer Res 2012; 72:4984–92.
26. Melnyk S, Pogribna M, Pogribny I, Hine RJ, James SJ. A new HPLC method for the simultaneous determination of oxidized and reduced plasma aminothiols using coulometric electrochemical detection. J Nutr Biochem 1999; 10:490–7.
27. Sridharan V, Tripathi P, Sharma S, Moros EG, Zheng J, Hauer-Jensen M, et al. Roles of sensory nerves in the regulation of radiation-induced structural and functional changes in the heart. Int J Radiat Oncol Biol Phys 2014; 88:167–74.
28. Oberley LW, Lindgren LA, Baker SA, Stevens RH. Superoxide lon as the cause of the oxygen effect. Radiat Res 1976; 68:320–8.
29. Biaglow JE, Mitchell JB, Held K. The importance of peroxide and superoxide in the X-ray response. Int J Radiat Oncol Biol Phys 1992; 22:665–9.
30. Spitz DR, Azzam EI, Li JJ, Gius D. Metabolic oxidation/reduction reactions and cellular responses to ionizing radiation: a unifying concept in stress response biology. Cancer Metastasis Rev 2004; 23:311–22.

31. Chatterjee A. Reduced glutathione: a radioprotector or a modulator of DNA-repair activity? Nutrients 2013; 5:525–42.

32. An J, Li P, Li J, Dietz R, Donath S. ARC is a critical cardiomyocyte survival switch in doxorubicin cardiotoxicity. J Mol Med (Berl) 2009; 87:401–10.

33. Brady NR, Hamacher-Brady A, Gottlieb RA. Proapoptotic BCL-2 family members and mitochondrial dysfunction during ischemia/reperfusion injury, a study employing cardiac HL-1 cells and GFP biosensors. Biochim Biophys Acta 2006; 1757:667–78.

34. Capano M, Crompton M. Bax translocates to mitochondria of heart cells during simulated ischaemia: involvement of AMP-activated and p38 mitogen-activated protein kinases. Biochem J 2006; 395:57–64.

35. Gustafsson AB, Tsai JG, Logue SE, Crow MT, Gottlieb RA. Apoptosis repressor with caspase recruitment domain protects against cell death by interfering with Bax activation. J Biol Chem 2004; 279:21233–8.

36. Makpol S, Abdul RN, Hui CK, Ngah WZ. Inhibition of mitochondrial cytochrome c release and suppression of caspases by gamma-tocotrienol prevent apoptosis and delay aging in stress-induced premature senescence of skin fibroblasts. Oxid Med Cell Longev 2012; 2012:785743.

37. Shimizu S, Narita M, Tsujimoto Y. Bcl-2 family proteins regulate the release of apoptogenic cytochrome c by the mitochondrial channel VDAC. Nature 1999; 399:483–7.

38. Halestrap AP, Clarke SJ, Javadov SA. Mitochondrial permeability transition pore opening during myocardial reperfusion–a target for cardioprotection. Cardiovasc Res 2004; 61:372–85.

39. Murphy E, Steenbergen C. Mechanisms underlying acute protection from cardiac ischemia-reperfusion injury. Physiol Rev 2008; 88:581–609.

40. Weiss JN, Korge P, Honda HM, Ping P. Role of the mitochondrial permeability transition in myocardial disease. Circ Res 2003; 93:292–301.

41. Fajardo LF, Eltringham JR, Steward JR. Combined cardiotoxicity of adriamycin and x-radiation. Lab Invest 1976; 34:86–96.

42. Finsterer J, Ohnsorge P. Influence of mitochondrion-toxic agents on the cardiovascular system. Regul Toxicol Pharmacol 2013; 67:434–45.

43. De OF, Chauvin C, Ronot X, Mousseau M, Leverve X, Fontaine E. Effects of permeability transition inhibition and decrease in cytochrome c content on doxorubicin toxicity in K562 cells. Oncogene 2006; 25:2646–55.

44. Nowak G, Bakajsova D, Hayes C, Hauer-Jensen M, Compadre CM. gamma-Tocotrienol protects against mitochondrial dysfunction and renal cell death. J Pharmacol Exp Ther 2012; 340:330–8.

45. Barjaktarovic Z, Schmaltz D, Shyla A, Azimzadeh O, Schulz S, Haagen J, et al. Radiation-induced signaling results in mitochondrial impairment in mouse heart at 4 weeks after exposure to X-rays. PLoS One 2011; 6:e27811.

46. Franken NA, Hollaar L, Bosker FJ, Van Ravels FJ, van der Laarse A, Wondergem J. Effects of in vivo heart irradiation on myocardial energy metabolism in rats. Radiat Res 1993; 134:79–85.

47. Barjaktarovic Z, Shyla A, Azimzadeh O, Schulz S, Haagen J, Dorr W, et al. Ionising radiation induces persistent alterations in the cardiac mitochondrial function of C57BL/6 mice 40 weeks after local heart exposure. Radiother Oncol 2013; 106:404–10.

48. Seemann I, Gabriels K, Visser NL, Hoving S, te Poele JA, Pol JF, et al. Irradiation induced modest changes in murine cardiac function despite progressive structural damage to the myocardium and microvasculature. Radiother Oncol 2012; 103:143–50.

49. Boerma M, Wang J, Wondergem J, Joseph J, Qiu X, Kennedy RH, et al. Influence of mast cells on structural and functional manifestations of radiation-induced heart disease. Cancer Res 2005; 65:3100–7.

50. Kruse JJ, Strootman EG, Wondergem J. Effects of amifostine on radiation-induced cardiac damage. Acta Oncol 2003; 42:4–9.

51. Tokatli F, Uzal C, Doganay L, Kocak Z, Kaya M, Ture M, et al. The potential cardioprotective effects of amifostine in irradiated rats. Int J Radiat Oncol Biol Phys 2004; 58:1228–34.

52. Ghobadi G, Van der Veen S, Bartelds B, De Boer RA, Dickinson MG, De Jong JR, et al. Physiological interaction of heart and lung in thoracic irradiation. Int J Radiat Oncol Biol Phys 2012; 84:e639–46.